

Article

Characters and Metallogenetic Significance of Organic Matter in Coal from the Daying Sandstone-Hosted Uranium Deposit in the Northern Ordos Basin, China

Qi Li ^{1,2} , Bailin Wu ^{1,*}, Jingjing Luo ¹, Songlin Yang ³, Miao Wang ^{1,2}, Mingyi Liu ¹, Zhouyang Lin ¹, Xiaorui Zhang ¹, Long Zhang ⁴, Jiangqiang Wang ¹ and Mengdi Yang ¹

¹ State Key Laboratory of Continental Dynamics, Department of Geology, Northwest University, Xi'an 710069, China

² Research Institute of Exploration and Development, PetroChina Changqing Oilfield Company, Xi'an 710021, China

³ Research Institute of Exploration and Development, PetroChina Liaohe Oilfield Company, Panjin 124010, China

⁴ College of Earth Science and Engineering, Xi'an Shiyou University, Xi'an 710065, China

* Correspondence: wubailin@nwu.edu.cn

Abstract: Coal is usually found in many sandstone-hosted uranium deposits in western China. However, it remains unclear whether coal organic matter is related to the mineralization of uranium in sandstone. In this study, the organic matter of coal containing lenticular carbon plant strips and carbon clastics was analyzed in different alteration zones in the Daying sandstone-hosted uranium deposit located in the northern Ordos Basin. According to geological and geochemical characters, Daying sandstone can be classified into three alteration zones: the oxidation zone, the transition zone, and the reduction zone. The results are as follows. Firstly, the maceral organic matter of the coal at Daying is mostly vitrinite, indicating the characters of humic coal. The maturity of the organic matter is low, which is in the transitional evolution stage of immature lignite or lignite-long-flame coal. Secondly, the kerogen is mainly type III (humic type), which can be easily transformed into humic acid with a strong adsorption capacity for uranium. Thirdly, the vitrinite reflectance (R_o) of the coal organic matter in the transition zone is higher than that of the other alteration zones. Meanwhile, there are bright white bands in the microscopic components of the organic matter of the coal in the transition zone (mineralized zone) and a certain composition of the sapropelite has strong fluorescence. All three aforementioned phenomena are related to the radioactivity of uranium, and each of them possesses the potential for application in mineral exploration. Fourthly, the extraction and separation of humic substances indicates that humic acid plays a key role in organic matter-related uranium mineralization. In the transition zone, uranium can co-precipitate as a humate, and the transition zone's organic carbon content increases. Therefore, the organic matter in coal contributes to sandstone-hosted uranium mineralization, providing a further guide to prospecting methodologies.

Keywords: sandstone-hosted uranium deposit; Daying; coal organic matter; vitrinite reflectance; sapropelite; fluorescence; bright white bands; radioactive hydrocarbon generation



Citation: Li, Q.; Wu, B.; Luo, J.; Yang, S.; Wang, M.; Liu, M.; Lin, Z.; Zhang, X.; Zhang, L.; Wang, J.; et al. Characters and Metallogenetic Significance of Organic Matter in Coal from the Daying Sandstone-Hosted Uranium Deposit in the Northern Ordos Basin, China. *Minerals* **2023**, *13*, 1002. <https://doi.org/10.3390/min13081002>

Academic Editor: David Quirt

Received: 2 June 2023

Revised: 19 July 2023

Accepted: 23 July 2023

Published: 28 July 2023



Copyright: © 2023 by the authors. Licensee MDPI, Basel, Switzerland. This article is an open access article distributed under the terms and conditions of the Creative Commons Attribution (CC BY) license (<https://creativecommons.org/licenses/by/4.0/>).

1. Introduction

In western China, the Ordos Basin is a sedimentary basin rich in coal, oil, natural gas, uranium, and other energy resources [1]. Recent years have seen China increase investment in the exploration of uranium resources, and large deposits of uranium have been discovered in the northern part of the Ordos Basin, such as the Dongsheng, Hangjinqi, and Daying uranium deposits [2] (Figure 1). The field survey revealed that these deposit-bearing seams are coal-bearing strata, with high gamma ray readings, and a large amount of organic matter in the core, such as carbonaceous fragments and lenticular carbonaceous

stripes. Specifically, the coal-bearing strata provide coal organic matter to the U-mineralized strata, while carbonaceous fragments have an adsorption or reduction effect on uranium. Some scholars believed that the coal-bearing strata provide reducing gas for uranium mineralization, while others held that the humus in the coal organic matter is responsible for uranium mineralization enrichment [3–17].

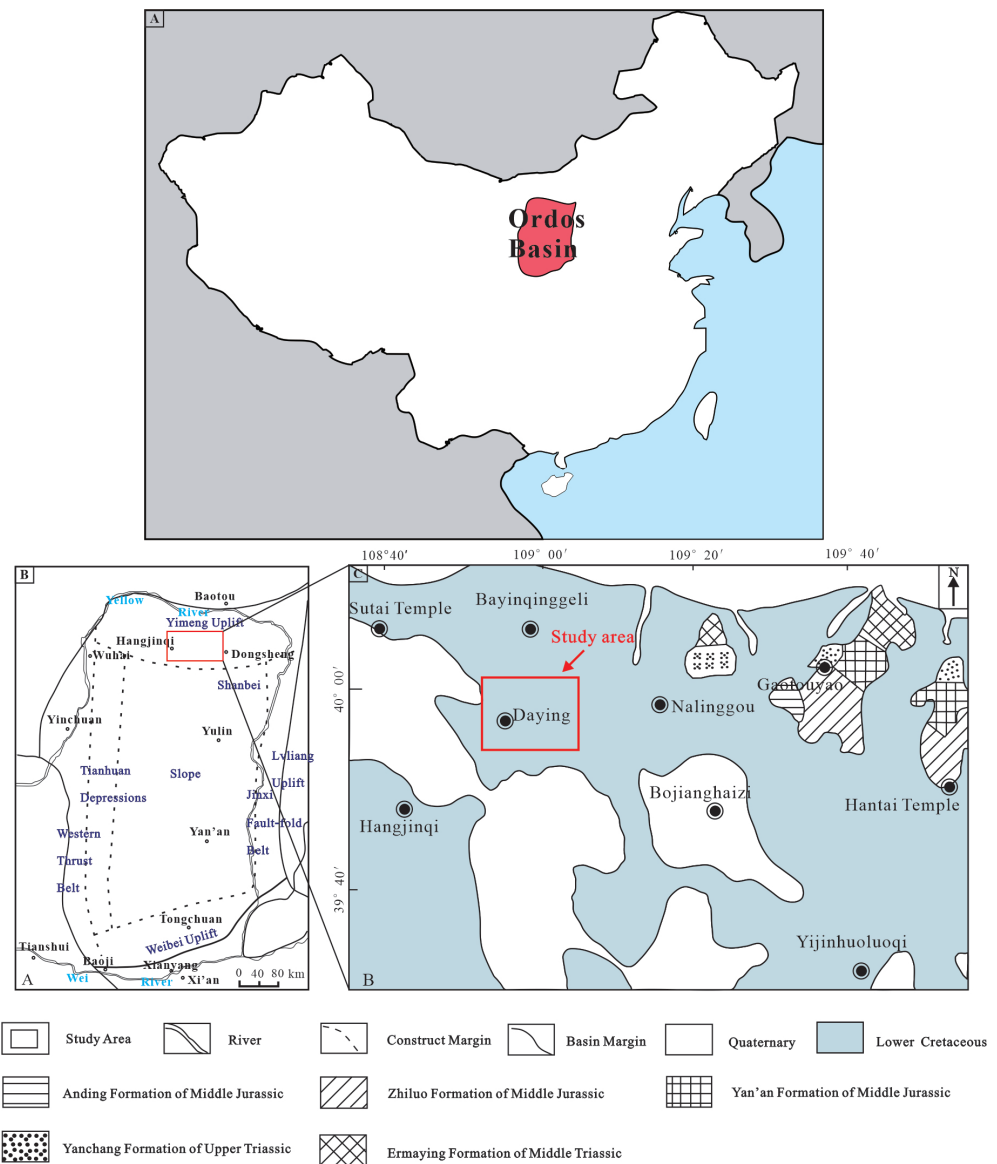


Figure 1. Regional geological map in the northern part of the Ordos Basin, China (modified after [18]). (A) = national-scale location map; (B) = topographic map; (C) = geological map.

Humic acid, the main component of humus [3], forms stronger coordination bonds with uranyl ions than weak acid carbonates in natural water [4,5,17]. The ability of solid humic acids to precipitate uranium as uranyl ions was also verified using infrared spectroscopy [9,19,20]. Simulating the coordination of coal in uranium mineralization revealed that most of the organic acid–uranyl complexes were stable in the air as well as in aqueous solutions. A further conclusion was that uranium migrates primarily as complexes in aqueous solutions [5,17]. After coal organic matter in the capacitated stratum is oxidized and decomposed in the oxidation zone, uranium–humic acid complexes are formed by humic acid and uranyl ions and are dissolved and migrated in the groundwater. As complexes enter the transition zone, uranium precipitates and becomes enriched in the form of

humate within an oxidation–reduction barrier in which the organic carbon is significantly increased [6–8,11–13,21,22].

The aforementioned work was primarily concerned with the effect of coal organic matter on the migration and precipitation of uranium in sandstone uranium mineralization under oxidizing–reducing conditions. Nevertheless, the relationship between organic matter characters and uranium mineralization in sandstone-hosted uranium deposits remains unclear and requires further study. In this study, the geological and geochemical characters of coal organic matter containing lenticular carbonaceous strips and carbonaceous fragments in sandstones from different alteration zones are examined. The relation between the characters of organic matter and uranium mineralization and enrichment is also clarified. The results will serve as markers and a basis for the discovery of sandstone-hosted uranium mineralization.

2. Geological Setting

The Daying uranium deposit is located in the Dongsheng area of the northern Ordos Basin [23] (Figure 1), where the Mesozoic strata were mainly developed, from old to new, in the Triassic, Jurassic, and Cretaceous, respectively. The lithology developed in the Triassic (T) is dominated by interbedded mudstones and sandstones, with thin coal seams locally interspersed, of which the Yanchang Formation (T_{3y}) is enriched with coal and petroleum. Jurassic (J) formations have developed from old to new, the Fuxian Formation (J_{1f}), Yan'an Formation (J_{2y}), Zhiluo Formation (J_{2z}), and Anding Formation (J_{2a}), among which the Fenfanghe Formation (J_{3f}) has not yet evolved. The Middle–Lower Jurassic is characterized by coal-bearing rock interbedded with sandy mudstone, whereas the Upper Jurassic is mainly characterized by gray-purple fine sandstone interbedded with gray-brown mudstone. It is evident that the Cretaceous (K) strata have been severely denuded and the Upper Cretaceous is absent from the basin. Only the Lower Cretaceous Zhidan Formation is relatively developed, characterized primarily by purple-red and gray-green sand conglomerates in angular unconformity contact with the upper and lower strata. Drilling in the study area has exposed the Yan'an Formation (J_{2y}), Zhiluo Formation (J_{2z}), and Anding Formation (J_{2a}) of the Middle Jurassic (Figure 2). As a result of the combination of longitudinal sandstone and siltstone contained in the Yan'an Formation, which contains a significant amount of oil and coal, it is interbedded with several coal seams and coal lines, with “bleached sandstone” (a kind of post-alteration sandstone) developing on top, which identifies the Zhiluo Formation overlying. The Fuxian Formation is integrated with or pseudo-integrated with this formation. The Zhiluo Formation, which is widely developed in the northern part of the basin, is the main U-mineralized strata in the study area, and the subject of this study. It is composed primarily of gray and gray-green sandstones, purple-red mudstones, and miscellaneous colored siltstones, with unconformable contact with the Yan'an Formation beneath. The lithology of the Anding Formation is mudstone, gray-green muddy sandstone, and purple-red fine sandstone, which are parallel unconformable to the underlying Zhiluo Formation (Figure 2).

The Daying uranium deposit belongs to the paleo-interstratified oxidized-zone sandstone type of uranium mineralization, resulting from groundwater containing oxidized U⁶⁺ at the surface, and the shallow oxidized zone is reduced to U⁴⁺ precipitation at an oxidation–reduction interface during downward migration along permeable sandstone layers and enrichment to produce mineralization [24]. Based on rock color and mineral geochemical zonation, this type of uranium deposit can be divided macroscopically into oxidation zones, transition zones, and reduction zones. Unlike the typical recent interstratified oxidation zone, the oxidation zone in the paleo-interstratified oxidized zone is modified by post-generation reduction and mainly appears green, lacking organic matter, such as carbon debris and pyrite. Meanwhile, residual traces of primitive paleo-oxidation are occasionally visible, specifically in the form of a small amount of dark yellowish-brown or reddish-brown sandstones, with large amounts of limonite or hematite; the transition zone consists of grayish-green rocks interspersed with gray rocks, containing large amounts

of pyrite; and the reduction zone consists of gray primary rocks. In conjunction with prior research [12,25–27], the Daying sandstone-type uranium deposit is associated with the braided river delta plain subphase sedimentation. The paleo-oxidation zone is dominated by braided river deposits, whereas the transition zone is dominated by braided river channel deposits, abandoned river channel deposits, and transgressive bank deposits. The transition zone sedimentary micro-phases primarily indicate a relatively weak hydrodynamic environment and generally stationary and reductive petrographic paleogeography. This is clearly distinct from the intense hydrodynamic and oxidation environment represented by the paleo-oxidation zone’s braided river sedimentary stages. As a result, the transition zone’s relatively stable, warm, and humid paleogeographic environment is better suited for the development and enrichment of organic matter. This also creates suitable circumstances for the conversion of organic matter into humus in the later transitional zone for the pre-enrichment of uranium mineralization.

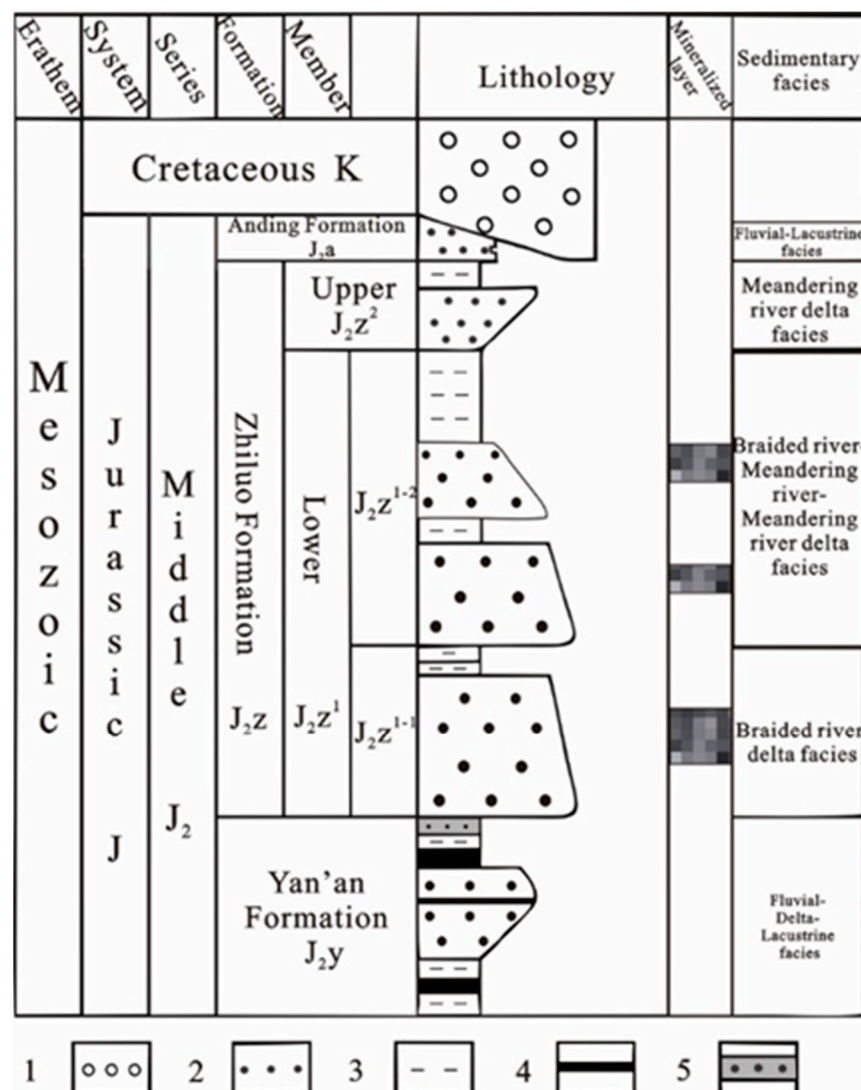


Figure 2. The stratigraphic section in the northern part of the Ordos Basin, China (modified after [18]). 1. Conglomerate; 2. sandstone; 3. mudstone; 4. coal layer; 5. kaolinized sandstone.

In this area, uranium mineralization occurs predominantly in the upper subsection (J_2z^{1-2}) of the lower section of the Middle Jurassic Zhiluo Formation, and there is no uranium mineralization in the upper section (Figure 2). As a result of the Yanshan movement (Jurassic Period) during the sedimentary period of the Zhiluo Formation, the paleotopography of the northern part of the Ordos Basin is generally higher in the northwest and

lower in the southeast [28,29]. In the meantime, the basin as a whole began to uplift, and the Yishan slope structure began to tilt moderately. These tectonic changes all indicate the onset of tectonic activation and interstratigraphic oxidation favorable to uranium mineralization [30], and this tectonic also determines the direction of groundwater runoff in the late Middle Jurassic, which is essentially consistent with the development of braided fluvial sedimentary sandstone bodies of the Zhiluo Formation [31]. The paleo-hydrodynamic condition of the “replenishment-trail-drainage” ancient groundwater is favorable for the formation of sandstone-hosted uranium deposits with interstratigraphic oxidation zones. During the Eocene–Miocene epoch, interstratigraphic oxidation gradually weakened, resulting in uranium precipitation, deposition, and enrichment (Figure 3). Afterward, the uranium deposits were further enriched and preserved by the secondary reduction in oil and gas [9,32–35].

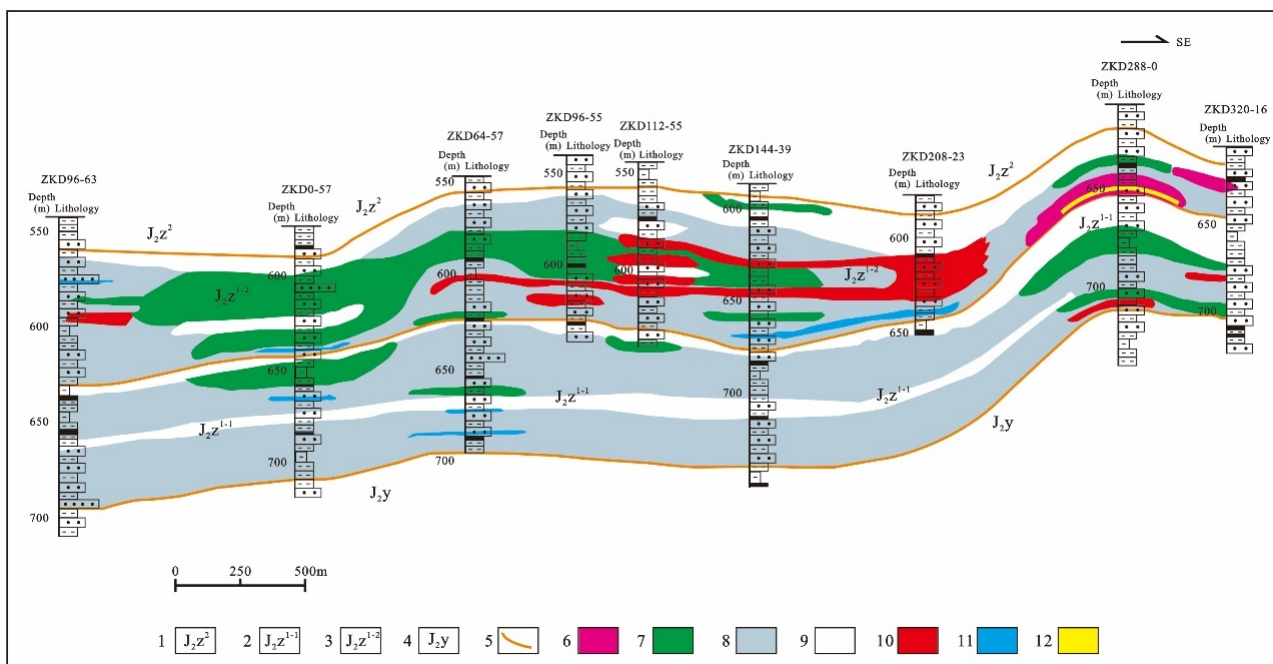


Figure 3. A southeast cross-section of the Daying sandstone-type uranium deposit. 1. The upper section of the Zhiluo Formation; 2. the upper subsection of the lower section of the Zhiluo Formation; 3. the lower subsection of the lower section of the Zhiluo Formation; 4. Yan’an Formation; 5. stratigraphic boundary; 6. purple-red sandstone; 7. green-grayish green sandstone; 8. gray sandstone; 9. mudstone–siltstone; 10. industrial-grade uranium mineralization body; 11. uranium mineralization; 12. uranium anomaly.

In the plane, the distribution of uranium mineralization is largely controlled by the gray-green-gray sand body, which is the green alteration zone (Paleo-interstratified oxidized zone). Unlike typical recent interstratified oxidation zones, which have a brilliant red (yellow) hue, the interstratified oxidation zone of the Daying uranium deposit has a paleo-interstratified oxidized zone of gray-green-gray sandstone [26]. Green sand bodies are believed to form from the ancient interstratified oxide zone after early oxidation and secondary reduction modifications of organic matter such as oil and gas at a later stage [6,36,37]. The contact area between the gray and green sand bodies is the most favorable zone for uranium enrichment. However, the light gray sandstone is mostly endowed with uranium mineralization, while the gray-green sandstone is only partially endowed. In the vertical direction, uranium mineralization is found in the transition zone between the gray-green (transition zone) and gray sand body (reduction zone), which is especially closer to the gray sand body (Figure 3). In general, the mineralization occurs at depths of 100 to 150 m, usually in the form of plates or rolls.

In the study of uranium-mineralized sandstones, it has been shown that the type of uranium minerals in this area is dominated by uraninite with small amounts of titaniferous uraninite and bituminous uraninite, and other minerals coeval with uranium minerals, including pyrite, titaniferous iron oxide, calcite, quartz and potassium feldspar, among others. A number of epigenetic alterations are associated with uranium mineralization including carbonation, chlorite, pyrite, and kaolinite and oxidation of organic matter. And during field survey sampling, a large number of lenticular carbonaceous bands and carbonaceous debris were observed in U-mineralized sandstones (Figure 4), suggesting that there may be an intrinsic link between the enrichment of uranium mineralization hosted in sandstones and the organic matter of coal in the study area.



Figure 4. Carbon plant debris and several lenticular carbon plant strips concentrated in the sandstones from the Daying sandstone-hosted Uranium deposit. (A) = Lenticular carbon plant strips in drilling ZKD105-12; (B) = lenticular carbon plant strips in drilling ZKD96-47; (C) = carbon plant debris in drilling ZKD96-47; (D) = lenticular carbon plant strips in drilling ZKD32-15-2; (E) = lenticular carbon plant strips in drilling ZKD2015-4; (F) = lenticular carbon plant strips in drilling ZKD96-47.

3. Samples and Methodology

3.1. Samples

For the purpose of understanding the relationship between coal organic matter and uranium mineralization, 35 sandstone samples were collected from the oxidation, transition, and reduction zones of the Daying sandstone-hosted uranium deposit and tested. Sample sizes ranged from muddy siltstone to coarse sandstone, and sample colors included brownish-red, gray, gray-green, and grayish-white, the vast majority of which were abundant in carbonaceous clasts and carbonaceous strips.

3.2. Methodology

In the following experiments, the geological and geochemical characters of coal organic matter were examined. Firstly, uranium and organic carbon contents were measured at China No. 203 Research Institute of Nuclear Industry, Xianyang. All the samples were crushed to a size of 200 mesh after the surface material was removed. The U-content testing conformed to the Chinese nuclear industry standard EJ/T550-2000 [38] using MUA laser-induced fluorometry. The samples were decomposed by nitric acid, hydrofluoric acid, and perchloric acid, and uranium was present in the solution in the state of uranyl ion (UO_2^{2+}). At pH 7–9, the UO_2^{2+} fluorescent reagent formed a stable complex that emitted green fluorescence with different peak wavelengths under the excitation of a pulsed laser from the MUA-type laser. The fluorescence intensity was proportional to the uranium content in the sample solution. The uranium content was then calculated directly by the standard addition method. The organic carbon content test was carried out following the Chinese geological and mineral industry standard DZ/T0279.27-2016 [39]. The specimens were initially decocted using the oil bath external heating process. The organic carbon in the specimens was then oxidized with sulfuric acid-potassium dichromate. After cooling, the residual $\text{K}_2\text{Cr}_2\text{O}_7$ was titrated with the standard solution of Fe^{2+} , and finally, the content of organic carbon in the specimens was calculated by the amount of potassium dichromate consumed.

Meanwhile, some samples were selected for making coal-polished sections. Afterward, both organic maceral and vitrinite reflectance R_o were measured by polarization microscope and HD photometer at the Xi'an Research Institute of the China Coal Science & Technology Group, Xi'an. The most intuitive method to identify organic maceral is microscopy. Organic macerals were identified by placing the prepared thin sections under a polarizing microscope, observing and identifying the microscopic shape and composition of the organic particles under natural light and fluorescence, and determining the different organic macerals with fluorescence characters and intensity. The method of microscopically determining the reflectance of vitrinite in coal was performed according to the Chinese national standard GB/T6948-2008 [40]. Under an oil-infused objective microscope, the reflected light (λ) perpendicular to the incident light in a limited area on the surface of the specular body profile was measured. The intensity of the reflected light ($\lambda = 546 \text{ nm}$) of the incident light was measured with a photoelectric converter and compared to the intensity of the reflected light of a standard substance with known reflectance under the same conditions.

Meanwhile, $\delta^{13}\text{C}$ and kerogen elements were determined by a stable isotope mass spectrometer and elemental analyzer at the Analytical Centre of the Institute of Exploration and Development, China Petroleum University, Beijing. The $\delta^{13}\text{C}$ test method was performed by first crushing the sample to less than 110 mesh, then treating it with HCl-HF to remove any inorganic carbon that might be contained in the sample, and finally placing the dried powder sample after treatment into a MAT253 stable isotope mass spectrometer to determine the $\delta^{13}\text{C}$ value of CO_2 gas (PDB standard). The kerogen elements analysis was performed with an Elementar Vario EL elemental analyzer. The sample was placed in a combustion tube and oxygen was introduced at a high temperature so that the organic matter was oxidized, and then the nitrogen was reduced and separated by the reduction tube and column, and measured with a thermal conductivity detector, after which the carbon and hydrogen elemental contents were determined with an external standard method. Yet, the oxygen element was determined separately by high-temperature cracking and separation of the sample, and the generated CO content was determined by the thermal conductivity detector, which in turn determined the elemental oxygen content with an external standard method.

Furthermore, humic acid extraction and separation experiments were performed to analyze the relationship between coal organic matter and uranium. All samples were crushed to a size of 100 mesh after the surface material was removed. To start, a mixed solution was prepared by mixing 0.1 N NaOH with 0.1 M $\text{Na}_4\text{P}_2\text{O}_7 \cdot 10\text{H}_2\text{O}$ in a volume

ratio of 1:1. After mixing the 100-mesh rock samples with the mixed solution at a solid–liquid ratio of 1:10, the mixture was extracted at room temperature. Immediately following extraction, the extract solution was acidified with 1 M dilute hydrochloric acid, washed with distilled water, and then centrifuged to separate and precipitate the humic acid. Finally, the isolated humic acid was frozen and dried using freeze–thaw technology. All the above experiments were performed at the Beijing Research Institute of Uranium Geology, Beijing.

4. Results

4.1. Geological Characters of Coal Organic Matters

4.1.1. Correlation of Uranium to Organic Carbon Contents

Organic matter can always be found in all the samples examined (Figure 4). Tests on organic carbon and uranium content in each alteration zone (Table 1) indicated that organic carbon is highly enriched, while uranium is highest in the transition zone (Table 1, Figure 5). In contrast, the oxidized zone has the lowest average organic carbon content and the lowest average uranium content. Therefore, organic carbon and uranium enrichment are positively correlated.

Table 1. Uranium and organic carbon content of each alteration sandstone in Daying uranium deposits.

Sample	Zoning	Lithologic Description	U ppm	orgC wt. %
ZKD112-96(3)	Oxidation zone	Brown-red middle-fine sandstone	5.54	0.05
ZKD112-96(4)		Brown-red middle-fine sandstone	11.2	0.06
D63-16		Gray-white middle-fine sandstone with carbonaceous strips	6.75	1.01
Average			7.83	0.37
ZKD96-47(2)	Transition zone	Gray-white medium sandstone with carbonaceous strips	3640	2.55
D32-63-4		Gray medium sandstone contains a small amount of carbonaceous debris	3590	1.10
ZKD80-39-2		Gray medium sandstone contains a small amount of carbonaceous debris	1680	0.48
ZKD96-47-1		Gray-white medium sandstone	1290	0.35
2014DY-27		Gray siltstone sandstone contains a small amount of carbonaceous debris	2101	0.75
ZKD128-81-6		Light gray medium sandstone	683	0.28
2014DY-31		Gray medium sandstone contains a small amount of carbonaceous debris	2315	0.81
ZKD208-15-1		Gray-green medium sandstone contains carbonaceous strips.	828	0.32
ZKD96-31-1		Light grayish-green coarse sandstone contains carbonaceous detritus	1700	0.57
ZKD112-47-2		Grayish-white coarse sandstone contains carbonaceous detritus.	8480	1.53
Average		3647.6	0.88	
ZKD144-71(8)	Reduction zone	Grayish-white medium sandstone	25.1	0.10
D127-55-1		Grayish-white middle-coarse sandstone contains carbonaceous strips	96.3	1.28
Average			60.7	0.69

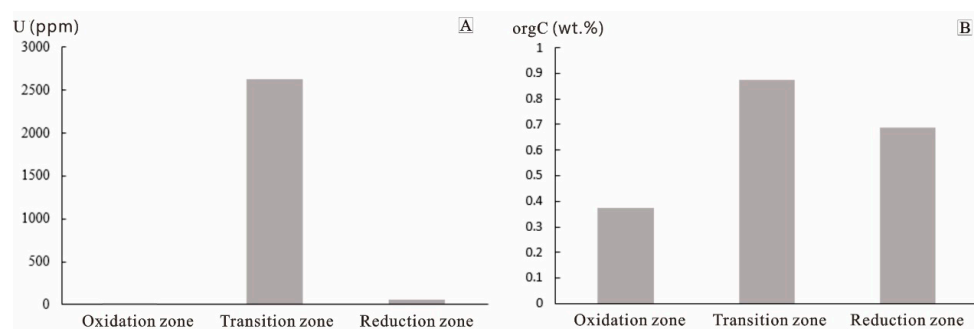


Figure 5. Uranium and organic carbon content of each alteration zone from the Daying uranium deposit. (A). Uranium content of alteration zone from the Daying uranium deposit; (B). organic carbon content of alteration zone from the Daying uranium deposit.

4.1.2. Organic Macerals

Coal organic matter in the study area is composed of three components (Table 2): vitrinite, which is the major component formed by woody plants under the reducing conditions; inertinite, which is also present and formed by woody plants under the oxidation conditions but has a low content; and exinite, which is primarily formed by horned skin, a

resin body, lipid, and pollen and is rare and commonly associated with pyrite. Vitrinite is the dominant component in all samples selected from each alteration zone, with a content of 94.5%–99.4%, reflecting the dominance of humus in continental coal. In contrast, the contents of exinite (0.0%–1.1%) and inertinite (0.0%–5.5%) are relatively low. The vitrinite content of humus coals is on average 96% or greater [41]. Therefore, it can be presumed that all coal chips found in the study area are humus coals.

In the organic maceral of mineralized sandstone, the microspore and cutinite show strong fluorescence (Figure 6A–D), indicating that the organic matter in mineralized sandstone has been influenced by late hydrocarbon action. Also, in the transition zone, bright white light is observed in the sample ZKD96-31-1 (Figure 6E,F), and this may be related to the high content of uranium in mineralized sandstone. It is hypothesized that radioactivity can change the structure and evolutionary degree of organic matter to cause this phenomenon. However, neither the non-mineralized oxidation zone nor the reduction zone exhibits these phenomena. Furthermore, some asphaltenes are also found to be present, which belong to the sapropel group.

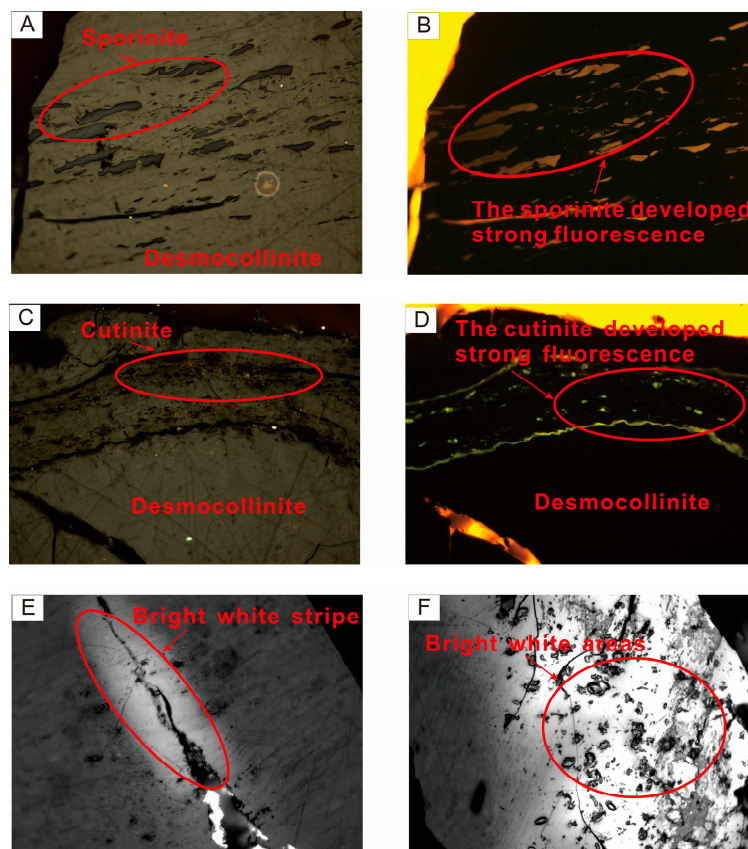


Figure 6. Microphotographs of maceral in coal's organic matter. (A) = Sporinite development of exinite. ZKD96-31-1 from transition zone in Daying uranium deposit; organic matter of coal rock chips $\times 500$ times. (B) = Sporinite in the exinite showing strong fluorescence; ZKD96-31-1 of the transition zone in Daying uranium deposit; organic matter of coal rock chips $\times 500$ times. (C) = Cutinite belt developed in desmocollinite; ZKD127-55-3 in the reduction zone of Daying uranium deposit; organic matter of coal rock chips $\times 500$ times. (D) = Cutinite belt developing strong fluorescence; ZKD127-55-3 of the reduction zone in Daying uranium deposit; organic matter of coal rock chips $\times 500$ times. (E) = Large bright white areas developed in the maceral; ZKD96-31-1 of reduction zone in Daying uranium deposit; organic matter of coal rock chips $\times 500$ times. (F) = Bright white stripes developed in the maceral; ZKD96-31-1 of reduction zone in Daying uranium deposit; organic matter of coal rock chips $\times 500$ times.

Table 2. Organic microcosmic components in Daying sandstone-hosted uranium deposits.

Sample	Zoning	Statistical Parameter	Organic Matter = 100%			Total	Maceral Description
			Vitrinite	Inertinite	Exinite		
D63-16	Oxidation zone	Number of measuring point	446	16	2	464	It is mainly telocollinite, pure and homogeneous, with a small amount of telinite. The fusinite, the microspore of the shell, and a small amount of asphaltene can be found. The fluorescence of asphaltene is very weak, and the illumination of the degree of metamorphism is very low.
		Percentage/%	96.1	3.5	0.4	100.0	
ZKD95-16-1	Oxidation zone	Number of measuring point	145	4	1	150	It is mainly telocollinite, which is transformed from the telinite, and the second is the telinite, which contains a small amount of the vitrinite. The semifusinite body develops and contains pyrite crystals, and the fluorescence of pyrite crystals is weak. It is indicated that pyrite crystals contain a small amount of bituminous bodies.
		Percentage/%	96.7	2.7	0.6	100.0	
ZKD96-31-1	Transition zone	Number of measuring point	266	11	3	280	It is mainly telocollinite, homogeneous and pure; the second is telinite. The development of the fusinite of inertinite. The sporinite of exinite with strong fluorescence.
		Percentage/%	95.0	3.9	1.1	100.0	
D32-63-4	Transition zone	Number of measuring point	87	12	1	100	It is mainly telocollinite and has a small amount of telinite, which contains small microsporophy of exinite and fusinite of inertinite.
		Percentage/%	87	12	1	100.0	
ZKD208-23-2	Transition zone	Number of measuring point	121	7	0	128	It is mainly homogeneous vitrinite, pure and homogenous, in which pyrite crystals are developed, and pyrite has a weak fluorescence. The fusinite of inertinite and inertoderinite was developed and the exinite was not developed.
		Percentage/%	94.5	5.5	0.0	100.0	
D127-55-1	Reduction zone	Number of measuring point	186	0	2	188	It is mainly homogeneous vitrinite, and a small amount of desmocollinite and telinite are developed. The cutinite of exinite and microsporinite was distributed in the desmocollinite, in which inertinite was not developed.
		Percentage/%	98.9	0.0	1.1	100.0	
D127-55-3	Reduction zone	Number of measuring point	173	0	1	174	It is mainly telocollinite, which contains pyrite crystals, and the pyrite contains the weak fluorescence of organic matter. We can see the desmocollinite and a small amount of telinite. The cutinite of exinite and microsporinite were distributed in the desmocollinite.
		Percentage/%	99.4	0.0	0.6	100.0	

4.1.3. Maturity of Organic Matter

The maturity of organic matter refers to the level of organic matter that gradually evolves and matures under the action of temperature and other energy conditions during deep burial. There are various parameters for determining the maturity of organisms, but among all of them, the vitrinite reflectance (R_o) is commonly used to determine an independent parameter for evaluating maturity because it is highly adaptable, highly reliable, and simple, and its determination is not affected by compositional changes. The criteria for judging the maturity of organic matter by vitrinite reflectance (R_o) are as in Table 3 (refer to the 1982 Standard of the Organic Geochemistry and Sedimentology Laboratory in the Institute of Geochemistry of the Chinese Academy of Sciences) [42].

Table 3. The criteria for judging the maturity of organic matter by vitrinite reflectance (R_o) [42].

Vitrinite Reflectance (R_o)	The Maturity of Organic Matter
$R_o < 0.5\%$	Immature stage
$R_o = 0.5\%–1.0\%$	Low-mature stage
$R_o = 1.0\%–1.35\%$	Medium-mature stage
$R_o = 1.35\%–2.0\%$	High-mature stage
$R_o > 2.0\%$	Over-mature stage

The vitrinite reflectance of the analyzed samples containing carbon plant debris and lenticular carbon plant strips from different alteration zones in the study area varies between 0.35% and 0.49% (Table 4), with an average R_o of 0.38, 0.43, and 0.36 for samples collected from the oxidation zone, transition zone, and reduction zone, respectively. Note that the vitrinite reflectance of the transition zone samples is relatively higher than that of the two other alteration zones. Corresponding to the three stages of the coal-forming process (peat-forming stage, lignite stage, bituminous coal or anthracite stage), the coal grade in the transition zone is higher than that in the oxidation and reduction zones and is in the lignite-long-flame coal (a kind of bituminous coal with a low degree of metamorphism) transition stage. Because the R_o of all the samples is less than 0.5%, the organic matter is in its immature stage. This indicates that the whole is in the lignite stage (immature coal rank), but the transition zone can also be in the lignite-long-flame coal transition stage.

Table 4. Reflectance data of vitrinite.

Sample	Lithologic Description	Zoning	Buried depth/m	R_o (%)	Standard Deviation	Maturity
D63-16	Gray-white middle-fine sandstone with carbonaceous strips.	Oxidation zone	630.5	0.38	0.034	
ZKD95-16-1	Light grayish-green sandstone with a lenticular carbonaceous strip.	Transition zone	606.00	0.39	0.033	Immature stage (lignite stage)
ZKD96-31-1	The grayish-green coarse sandstone contains carbonaceous detritus.		669.46	0.40	0.030	
D32-63-4	Gray medium sandstone contains a small amount of carbonaceous debris.		685.00	0.43	0.032	
ZKD208-23-2	Light grayish-green medium sandstone with a lenticular carbonaceous strip.		626.74	0.49	0.038	
D127-55-1	Grayish-white middle-coarse sandstone contains carbonaceous strips.	Reduction zone	594.10	0.35	0.029	
D127-55-3	The grayish-green medium sandstone contains carbonaceous strip.		626.35	0.37	0.018	

4.2. Geochemical Characters of Coal Organic Matter

4.2.1. Kerogen Types—Carbon Isotopes

The carbon isotopic composition of organic matter is determined by a combination of isotope differences between isotopes of the biogenic parent material and those produced by anadiagenesis. In general, different types of biocarbon isotopes have certain differences:

when the content of $\delta^{13}\text{C}$ is between -26‰ and -33‰ , its parent material is mostly lower plants, such as plant lipids, plankton, and algae; when the content of $\delta^{13}\text{C}$ is between -20‰ and -28‰ , its organic parent material is mostly terrestrial higher plants, lignin and cellulose. Currently, carbon isotopes are more commonly used to identify organic matter. In order to determine the $\delta^{13}\text{C}_{\text{VPDB}}$ of the kerogen, samples containing lenticular carbon strips and carbon debris (known as coal's organic matter) were collected from three different alteration zones of the Daying uranium deposit. The classification of organic matter types [42] (Table 5), which is based on the 1982 Standard of Organic Geochemistry and Sedimentology of the Institute of Geochemistry of the Chinese Academy of Sciences, is listed in Table 5. And the experimental results are shown in Table 6.

Table 5. Classification of organic matter types [42].

The Content of $\delta^{13}\text{C}$	Organic Matter Type
$\delta^{13}\text{C} < -28\text{‰}$	Type I (sapropel)
$\delta^{13}\text{C} = -28\text{‰}--26\text{‰}$	Type II ₁ (humic-sapropel)
$\delta^{13}\text{C} = -26\text{‰}--24\text{‰}$ or -24.5‰	Type II ₂ (sapropelic-humic type)
$\delta^{13}\text{C} > -24\text{‰}$ or -24.5‰	Type III (humic type)

Table 6. $\delta^{13}\text{C}$ data of kerogen (‰).

Sample	Lithologic Description	Zoning	Depth/m	Kerogen $\delta^{13}\text{C}\text{‰}$ (PDB)
ZKD112-96(3)	Brown-red middle-fine sandstone	Oxidation zone	691.67	-23.7
D63-16	Gray-white middle-fine sandstone with carbonaceous strips		630.50	-23.2
ZKD208-23-2	Gray-green sandstone contains a lenticular carbonaceous strip	Transition zone	626.74	-22.7
D32-63-4	Gray medium sandstone contains a small amount of carbonaceous debris		685.00	-21.5
ZKD95-16-1	Gray-green sandstone contains a lenticular carbonaceous strip		606.00	-22.5
ZKD208-15-1	Gray-green medium sandstone contains carbonaceous strips		625.00	-19.2
ZKD144-71(3)	Gray-green siltstone contains carbonaceous clastic and pyrite nodules	Reduction zone	614.47	-23.1
D127-55-1	Grayish-white middle-coarse sandstone contains carbonaceous strips		614.24	-23.6
D127-55-3	Gray-green middle-fine sandstone with carbonaceous strips		626.74	-24.2

The $\delta^{13}\text{C}$ values of the kerogen in the samples from each alteration zone in the study area are higher than -24‰ , except in sample D127-55-3 in which the $\delta^{13}\text{C}$ value is 24.2‰ (Table 6), indicating that the kerogen of the organic matter in the coal is mainly type III (humic type) and its organic parent material is mostly terrestrial higher plants.

4.2.2. Kerogen Chemistry

The ratio of the composition of kerogen elements to their atomic number can be used to determine the biological inputs and the type of organic parent material. Landais [18] found that lower aquatic organisms, such as bacteria and algae, are rich in protein, fat, and waxy amyllum, along with high contents of C and H, low content of O, and a high H/C ratio. Typically, the H/C atomic ratio ranges from 1.25 to 1.75, and the O/C original ratio ranges from 0.026 to 0.12. In contrast, lignin and cellulose in higher plants are rather concentrated in O but have very low levels of H, with low H/C ratios. And the H/C atomic ratio ranges from 0.46 to 0.93, and the O/C original ratio ranges from 0.05 to 0.30. The diagram of the H/C and O/C atomic number ratios in the elemental composition of kerogen is an effective method to identify the type of organic matter evolution and the

evolutionary environment, which is particularly useful for the identification of organic matter at low evolutionary stages.

According to Table 7, the elemental analysis of coal organic matter indicates high oxygen content but low hydrogen content of the elemental composition of kerogen. The H/C atomic ratio ranges from 0.67 to 0.85, while the O/C ratio ranges from 0.14 to 0.29. This indicates that its organic parent material is most likely higher plants. The distribution of the above test data in the H/C-O/C diagram is shown in (Figure 7), and the data points almost all fall within the type III (humic type) evolution zone, which indicates that the kerogen in all the samples analyzed is type III (humic type) and its sedimentation occurred in the deep burial epigenetic stage. Moreover, as indicated by the nearly horizontal linear trend (Figure 7) and the similar H/C ratios, there is not much difference in the types of organic matter.

Table 7. Elemental analysis of kerogen.

Sample	Lithologic Description	N%	C%	Test Project		H/C	O/C
				H%	O%		
ZKD112-96(3)	Brown-red middle-fine sandstone	0.23	59.26	3.95	23.54	0.79	0.29
D63-16	Gray-white middle-fine sandstone with carbonaceous strips	0.85	64.32	4.18	15.43	0.78	0.18
ZKD208-23-2	Gray-green sandstone contains a lenticular carbonaceous strip	0.90	67.84	3.82	12.51	0.67	0.14
D32-63-4	Gray medium sandstone contains a small amount of carbonaceous debris	0.14	53.28	3.18	12.65	0.72	0.18
ZKD95-16-1	Gray-green sandstone contains a lenticular carbonaceous strip	0.66	48.53	3.33	12.70	0.82	0.20
ZKD208-15-1	Gray-green medium sandstone contains carbonaceous strips	0.59	56.20	3.13	11.53	0.67	0.15
ZKD144-71(3)	Gray-green siltstone contains carbonaceous clastic and pyrite nodules	1.03	66.48	4.74	14.01	0.85	0.16
D127-55-1	Grayish-white middle-coarse sandstone contains carbonaceous strips	0.80	64.16	4.34	13.04	0.81	0.15
D127-55-3	Gray-green middle-fine sandstone with carbonaceous strips	0.81	63.22	4.39	13.90	0.83	0.16

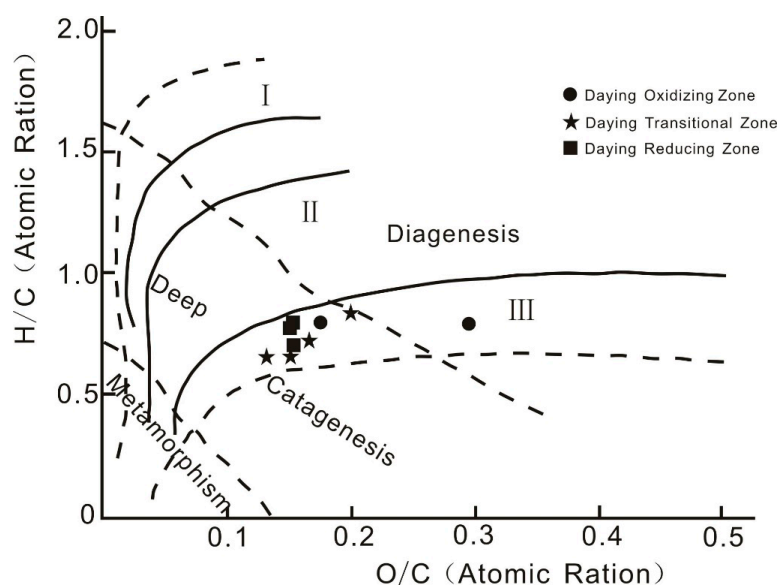


Figure 7. Distribution of H/C-O/C ratios. I is organic matter Type I; II is organic matter Type II; III organic matter Type III.

4.3. Analysis of Humic Acid and Uranium Content

The uranium content in the sandstone samples containing organic matter from different alteration zones, humic acid content, uranium content in humic acid, and uranium content in residue after humic acid extraction were also measured through humic acid extraction and isolation experiments (Table 8, Figure 8). According to the test data, organic matter controls uranium enrichment, particularly when humic acid is present. When humic acid is extracted from the sample, the major portion of the uranium is also taken out, resulting in a significant reduction of the uranium content of the residue. And the larger the proportion of humic acid, the smaller the uranium content in the residue after humic acid extraction. This indicates that humic acid in organic matter is closely related to uranium mineralization.

Table 8. Humic acid and uranium contents.

Sample	Lithologic Description	Zoning	Humic Acid (%)	U (μg/g)	The Uranium Content in the Residue after the Extraction of Humic Acid (μg/g)	The Uranium Content of Humic Acid (μg/g)
D63-16	Gray-white middle-fine sandstone with carbon strips	Oxidation zone	0.05	25.6	11.7	13.9
D112-96(4)	Brown-red middle-fine sandstone		0.27	137.5	51.7	85.8
D96-31(1)	Gray-green coarse sandstone contains carbonaceous debris	Transition zone	0.10	1231	480	751
D112-47(2)	Gray-white coarse sandstone contains carbonaceous debris		0.02	3933	943	2990
D32-63-4	Gray medium sandstone contains a small amount of carbonaceous debris		0.83	5030	595	4435
ZKD95-16-1	Gray-green sandstone contains a lenticular carbon strip		5.54	5085	672	4413
ZKD208-15-1	Gray-green medium sandstone contains carbon strips		1.13	96.2	20	76.2
ZKD144-71(3)	Gray-green siltstone contains carbonaceous clastic and pyrite nodules	Reduction zone	0.02	17.5	6.17	11.33
ZKD127-55-1	Grayish-white middle-coarse sandstone contains carbonaceous strips		2.07	1127	112	1015

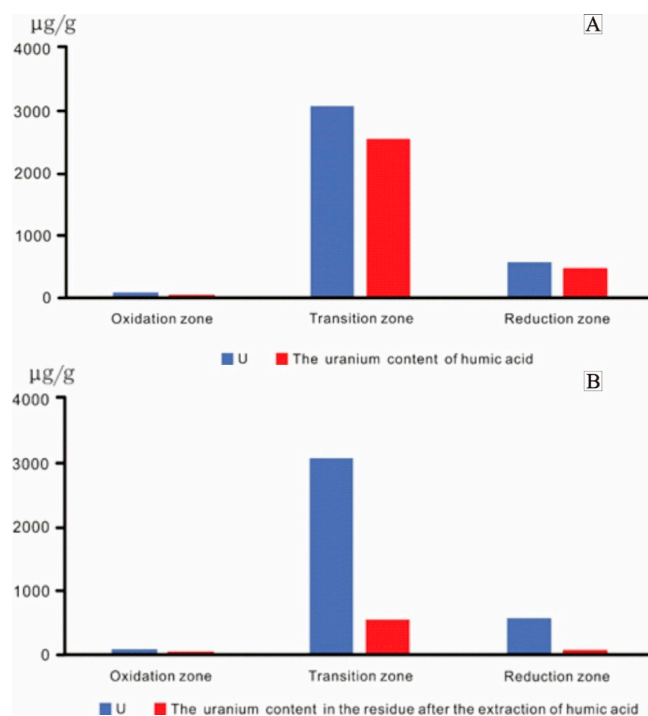


Figure 8. Comparison of the average U content of each alteration zone sample. (A). Uranium content in each alteration zone and uranium content in humic acid; (B). uranium content in each alteration zone, before and after the extraction of humic acid.

5. Discussion

5.1. Immature Organic Matter

At Daying, the primary component of organic maceral in coal is vitrinite, reflecting the characteristics of humus coal and equivalent to that in the lignite evolutionary stage. Because all the samples from the three alteration zones had an $R_o < 0.5\%$, it indicates that the organic matter is in the immature stage, which means that the overall evolution degree of organic matter is relatively low, and overall, it is in the lignite stage. Furthermore, the R_o of the transition zone samples is relatively higher than that of the two other alteration zones, which means the maturity of the organic matter in the transition zone is higher than that of the other two alteration zones. Therefore, organic matter in the transition zone is mainly in the transition stage of lignite-long-flame coal, while that in the oxidation zone and reduction zone is in the lignite stage. This phenomenon is caused by the radioactivity and thermogenesis of uranium, which contribute to the maturation of organic matter in the transition zone where sandstone-hosted uranium mineralization is predominantly enriched. Mao's articles [43–45] provide experimental support for this viewpoint.

The kerogen of organic matter in coal is mainly type III (humic type) and at a very low maturity level, which suggests that this organic matter is equivalent to the immature organic matter in lignite. This kind of organic matter is loose, porous, and has a large specific surface area. It is also frequently enriched with some active functional groups, such as OH, COOH, CO, and NH_2 . It is easy to convert into humic acid, which has a strong adsorption capacity and is conducive to uranium enrichment. In addition, kerogen chemistry indicates that coal organic matter is sourced from terrestrial higher plants and its sedimentation occurred during the deep burial epigenetic stage.

5.2. Relationship between Strong Fluorescence Properties and Uranium Mineralization

Strong fluorescence is observed from microspores and cutinite in organic maceral in coal in the transition zone (mineralized zone), indicating the presence of hydrocarbon components, while there is no fluorescence or only weak fluorescence in the unmineralized oxidation and reduction zones. This suggests that radioactive uranium enhances the hydrocarbon display or locally contributes to hydrocarbon generation due to the enrichment of uranium in the mineralized zone.

An elemental analysis of kerogen shows that the evolution of organic matter in this area occurred during the deep burial epigenesis period, indicating that there may be weak hydrocarbon generation from the organic matter. But why is there strong fluorescence observed only in the transition zone with uranium mineralization, and not in the oxidation and reduction zones without mineralization, or is this phenomenon weak?

According to Wu (2005) [46], a detailed coal petrographic study at the Zaohuohao uranium deposit in the eastern area of the Daying sandstone-hosted uranium deposit of the Dongsheng area found some obvious sapropelinite components locally in samples with higher uranium mineralization. The results are shown in Table 9. More than 90% of the organic maceral components of the coal chips in this area are composed of humus (vitrinite is dominant) formed by higher plants of carbonaceous chips or coal chips, mostly with characteristic cracks of vitrain. However, there is still about 2%–5% of sapropelinite (Figure 9), which shows strong fluorescence. The presence of sapropelinite, an important hydrocarbon-producing organic microcomponent, leads to strong fluorescence, and also suggests that the fluorescence phenomena are related to hydrocarbon interaction.

Based on the thermal simulation of hydrocarbon generation conducted by Mao [43–45], the application of sandstone-type uranium mineralization to various hydrocarbon source rocks resulted in hydrocarbon simulation products exhibiting enhanced maturity features in terms of group composition, saturated hydrocarbon gas chromatography, biomarker compounds, and other relevant parameters. The findings suggest that uranium has the ability to enhance the maturation of organic matter and reduce the hydrocarbon threshold in hydrocarbon source rocks. This facilitates the early generation of low-maturity hydrocarbons in source rocks. This observation further substantiates the role of organic matter

adsorption and the reduction environment in facilitating the enrichment and formation of diverse energy minerals, including uranium. Moreover, it highlights the impact of uranium on the hydrocarbon evolution process of hydrocarbon source rocks.

Table 9. Organic Matter Veinlets Composition of Higher Uranium Mineralization in Zaohuohao Uranium Mine (cited from Wu, 2005 [46]).

No.	Percentage (Organic Matter = 100%)				Description of Organic Components
	Vitrinite	Inertinite	Exinite	Sapropelinite	
Wd04-5	94.7	2.1	0.0	3.2	Mainly telocollinite, with a small amount of desmocollinite and semifusinite. The symbiosis between asphaltene and pyrite can be found.
Wd04-95	95.1	0.0	0.5	4.4	Mainly telocollinite and desmocollinite. Fusinite can be found with sporophyte and resinite. Abundant asphaltene is developed in fine striations in symbiosis with pyrite and clay or distributed in desmocollinite.
Wd04-103	84.7	8.5	3.4	3.4	Mainly telocollinite and desmocollinite with abundant telinite, semifusinite, and fusinite. The exinite is cutinite and sporophyte. And asphaltene can be found.
Wd04-108	87.3	10.2	1.5	1.0	Mainly telocollinite and desmocollinite, with abundant structural vitrinite, semifusinite, and fusinite. The exinite is cutinite and sporophyte. And asphaltene can be found.
Wd04-109	91.7	1.0	3.1	4.2	Mainly non-telocollinite with pyrite and abundant endogenous fissures. Fusinite can be found with sporophyte, cutinite, and sporophyte. Telocollinite is dark gray and may adsorb asphaltene.
Wd04-111	98.6	0.0	0.7	0.7	Mainly telocollinite with an amorphous flocculent distribution; a few desmocollinite and telinite with sporophyte and cutinite. Semifusinite and inertodetrinite can be seen, with asphaltene distribution.
Wd04-129	93.7	0.0	1.6	4.8	Mainly telocollinite with abundant endogenous fissures; a few desmocollinite and telinite with sporophyte, cutinite, and asphaltene. Telocollinite is dark gray and may adsorb asphaltene.
Wd04-138	93.5	1.1	2.2	3.2	Mainly telinite with abundant endogenous fissures, and structureless vitrinite is less frequent. Inertodetrinite, secretinite, and semifusinite fragments can be found, and asphaltene is present.
<i>Average</i>	92.4	2.9	1.6	3.1	

Note: The testing unit is China Coal Science and Industry Group, Xi'an Research Institute Co., CHN.

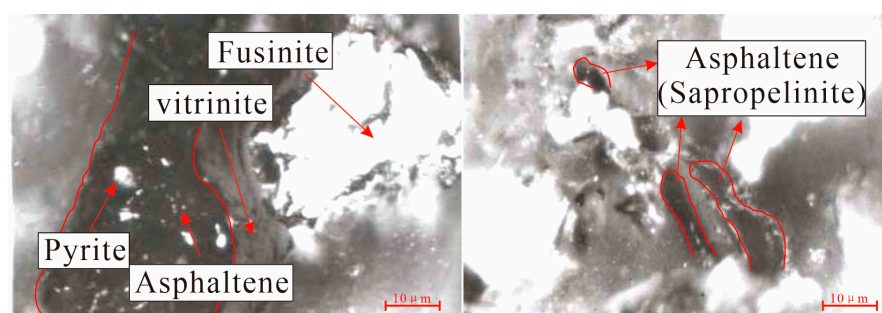


Figure 9. Thin section of organic vein coal (cited from Wu, 2005 [46]). W04-138, 306x, Zaohuohao Uranium Mine.

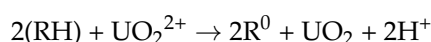
This phenomenon can be attributed to the influence of uranium mineralization in the transition zone, where the radioactivity of uranium plays a significant role in enhancing the maturity of organic matter and the formation of the humus group. Consequently, the radioactivity of hydrocarbon production lags, resulting in the manifestation of three distinct phenomena: strong fluorescence, obvious bright white stripes, and higher organic matter maturity.

5.3. Role of Organic Matter during Uranium Mineralization

The positive correlation between organic carbon and uranium content, both of which are very high in the transition zone, indicates that organic matter could play an important role in uranium enrichment (Figure 8). Firstly, we believe that higher organic carbon levels in the transition zone may be due to two factors. One is that the transition zone has braided river channels, abandoned river channels, and transgressive bank deposits, which exhibit relatively stable and weak hydrodynamic paleogeography, and such favorable environmental conditions are conducive to the growth and enrichment of organic matter. Another factor might be the accumulation of organic matter (humic acid) carried by interstratified water [34]. Uranyl–humic acid complexes are created when humic acids from organic matter from exotic sources combine with uranyl ions in oxygenated uranium-containing water in a weakly acidic environment. These complexes are then reduced to create precipitation enrichment in the transition zone with the continuous transport of interstratified water. This suggests that the oxidation–reduction geochemistry of uranium by humic acid is primarily responsible for the rise in the organic matter content of coal in the transition zone (mineralized zone).

Furthermore, the extraction and separation experiments of humus from the organic matter of coal revealed that the humic acid fraction in them is primarily responsible for uranium reduction and mineralization. The uranium content of the humic acid in the reduction zone should be the initial uranium content. And the uranium content of the humic acid in the oxidation zone is less than that in the transition zone, which might have been influenced by oxidation. In the oxidation zone, uranium lost from humic acid, probably including uranium from other components in the rocks, is washed, filtered (activated), and migrates in two directions. Some uranium (UO_2^{2+}) is immobilized by humic acid ($-\text{COOH}$ and $-\text{COO}^-$) during the migration period, and the other migrates downward to the transition zone and is re-enriched in humic acid.

In the uranium enrichment period, the organic matter in the oxidation zone is firstly destroyed and decomposed to produce gases such as H_2S , H_2 , and CH_4 or other decomposition products. They can reduce UO_2^{2+} to UO_2 , and this is the reason why the organic matter of coal can act as a reductant for uranium mineralization. This process can be represented by the following chemical reaction formula [47].



Next, the soluble uranyl–humic acid complexes are formed by UO_2^{2+} and $-\text{COOH}/-\text{COO}^-$ and leached into groundwater for forward transport. The chemical reaction formula can be expressed as follows [48].



Then, they are deposited in the transition zone as uranium humate, which could explain the increase in the organic carbon content in the transition zone. Similar conclusions have been reached in previous studies on the Shihongtan deposit in the Tuha Basin [8,9,19].

6. Conclusions

- (1) The ore of the Daying uranium mine usually contains lots of coal organic matter which is positively correlated to uranium enrichment. The primary maceral of coal organic matter is mostly vitrinite, reflecting the characters of humic coal. And the organic matter is in the immature stage, which is equivalent to immature lignite or the lignite-long-flame coal stage, due to an $\text{R}_o < 0.5\%$.
- (2) The organic matter in coal at Daying is dominated by type III (humic type) kerogen. This kind of organic matter has a strong adsorption capacity for uranium and acts as a reductant in uranium enrichment and mineralization. The humic acid in the coal organic matter plays an important role in uranium mineralization, as evidenced by humic substance extraction and separation experiments. In the transition zone,

uranium was precipitated in the form of uranium humate, and the organic carbon content in the transition zone increased. Kerogen chemistry shows that coal organic matter is sourced from terrestrial higher plants and its sedimentation occurred during the deep burial epigenetic stage, which was strongly influenced by epigenesis, fluids, and natural gas.

- (3) The vitrinite reflectance (Ro) of the coal is relatively higher in the transition zone (mineralized zone) than that in the reduction and oxidation zones. The phenomenon can be attributed to the catalytic influence of uranium mineralization on organic matter, leading to a marginally greater degree of organic matter maturation compared to other zones. Furthermore, it can serve as a definitive indication of mineral exploration.
- (4) In the transition zone (mineralized zone), the microspore and cutinite of the organic matter exhibit strong fluorescence (hydrocarbon shows) and bright white bands in the organic maceral components. These can also be utilized for the purpose of mineral exploration. These phenomena are associated with the radioactive properties of uranium and the impact of hydrocarbons. The phenomenon of fluorescent localized sapropelinite can be attributed to the localized enrichment of uranium within the organic matter, resulting in enhanced maturation of the organic matter and early generation of hydrocarbon production.

Author Contributions: Conceptualization, J.L.; methodology, Q.L. and J.L.; software, M.W. and J.W.; validation, L.Z.; formal analysis, Z.L. and X.Z.; investigation, M.L.; resources, S.Y.; data curation, J.L.; writing—original draft preparation, Q.L.; writing—review and editing, Q.L. and B.W.; visualization, M.Y.; supervision, B.W.; project administration, B.W.; funding acquisition, S.Y. and M.L. All authors have read and agreed to the published version of the manuscript.

Funding: This research was funded by the Natural Science Basic Research Program (Key) Project of Shaanxi Province, China grant number 2022JZ-18, the China Geological Survey Project grant number DD20211550, the Science and Technology Project of PetroChina Liaohe Oilfield Company grant number 2021DJ5301, and the Uranium Resource Potential and Techno-Economic Evaluation Project in Central Kyzyl-Kum Region, Uzbekistan, Key R&D Program of Shaanxi Province, China grant number 2021KW-28.

Data Availability Statement: All data generated and analyzed during this study are included in this published article.

Acknowledgments: Financial support of this study by the Natural Science Basic Research Program (Key) Project of Shaanxi Province, China (Grant No. 2022JZ-18), the China Geological Survey Project (Grant No. DD20211550), the Science and Technology Project of PetroChina Liaohe Oilfield Company (Grant No. 2021DJ5301), and the Uranium Resource Potential and Techno-Economic Evaluation Project in Central Kyzyl-Kum Region, Uzbekistan, Key R&D Program of Shaanxi Province, China (Grant No. 2021KW-28) is gratefully acknowledged.

Conflicts of Interest: The authors declare no conflict of interest.

References

1. Liu, C.Y.; Zhao, H.G.; Gui, X.J.; Yue, L.P.; Zhao, J.F.; Wang, J.Q. Space-Time Coordinate of the Evolution and Reformation and Mineralization Response in Ordos Basin. *Acta Geol. Sin.* **2006**, *5*, 617–638, (In Chinese with English abstract).
2. Jin, R.S.; Miao, P.S.; Sima, X.Z.; Feng, X.X.; Tang, C.; Zhu, Q.; Li, G.Y. Discussion on the classification about the uranium deposit. *Geol. Surv. Res.* **2014**, *37*, 1–5.
3. Charles, S. The roles of organic matter in the formation of uranium deposit in sedimentary rock. *Ore Geol. Rev.* **1996**, *11*, 54–55.
4. Shanbhag, P.M. Binding of uranyl by humic acid. *Nucl. Chem.* **1981**, *43*, 41–54. [[CrossRef](#)]
5. Wood, S.A. The role of humic substances in the transport and fixation of metals of economic interest (Au, Pt, U, V). *Ore Geol. Rev.* **1996**, *11*, 2–6. [[CrossRef](#)]
6. Wu, B.L.; Liu, C.Y.; Wang, J.Q. Basical Characters of Fluid Geologic process of Interlayer Oxidation Zone Standstone-hosted Uranium Deposit. *Sci. China Ser. D Earth Sci.* **2007**, *50*, 185–194. [[CrossRef](#)]
7. Wu, B.L.; Xu, G.W.; Liu, C.Y.; Qiu, X.W.; Wang, J.Q.; Hu, L.; Zhang, B.H. Alteration Effects of Hydrocarbon Dissipation in the Dongsheng Uranium Deposit, The Ordos Basin—Explanation for Green Alteration and Bleaching Phenomenon. *Energy Explor. Explor.* **2009**, *27*, 181–199.

8. Xiang, W.D.; Chen, Z.B.; Chen, Z.Y.; Yin, J.S. Discussion on the mineralization of organic matter and epigenetic sandstone-hosted uranium deposit—a case study of Shihongtan area in the Tuha basin. *Uranium Geol.* **2000**, *16*, 65–114.
9. Xiang, W.D.; Yin, J.S. The mechanism of humic acid in the mineralization process of sandstone-type uranium deposit. *World Nucl. Geol.* **2006**, *23*, 73–77.
10. Xiang, W.D.; Fang, X.Y.; Li, T.G.; Chen, X.L.; Pang, Y.Q.; Cheng, H.H. Metallogenic characters and metallogenic model of Dongsheng uranium deposit in northeastern the Ordos Basin. *Uranium Geol.* **2006**, *22*, 257–265.
11. Qiao, H.M.; Song, Z. Study on the interaction of microorganism and organic matter in uranium mineralization process of Shihongtan uranium deposit in the Tuha Basin. *Ore Geol. Rev.* **2015**, *61*, 229–236.
12. Sun, Y. The organic geochemical zonation of sandstone uranium deposit and its relationship with uranium mineralization—A case study of the Zaohuohao uranium deposit in Inner Mongolia. *Uranium Geol.* **2016**, *32*, 129–136.
13. Zhang, L.; Wu, B.L.; Liu, C.Y.; Lei, K.Y.; Hou, H.Q.; Sun, L.; Cun, X.N.; Wang, J.Q. Province Source Analysis of Zhiluo Formation of Sandstone-hosted Uranium Deposit in North the Ordos Basin and Its Uranium Mineralization Significance. *Acta Geol. Sin.* **2016**, *90*, 3441–3453.
14. Zhu, Q.; Yu, R.A.; Li, J.G.; Sima, X.Z.; Si, Q.H.; Li, G.Y.; Wen, S.B.; Liu, X.X.; Wang, S.B. Pairs of Reducing Media in the Tarangaole Area in the Northeastern Part of the Ordos Basin Control of Sandstone-Type Uranium Deposits. *Coal Geol. Explor.* **2018**, *46*, 11–18.
15. Jiao, Y.Q.; Wu, L.Q.; Rong, H. The Dual Reducing Medium Model of Sandstone-Type Uranium Deposits and its Joint Ore-Controlling Mechanism: A Discussion on the Daying and Qianjiadian Uranium Deposits. *J. Earth Sci.* **2018**, *43*, 459–474.
16. Zhu, Q.; Yu, R.A.; Li, G.Y.; Wen, S.B.; Li, J.G.; Si, Q.H.; Guo, H. Associated Minerals of Sandstone-Type Uranium Deposits in the Northeast of Ordos Basin and Their Geological Significance. *Geotecton. Metallog.* **2021**, *45*, 327–344.
17. Landais, P. Organic geochemistry of sedimentary uranium ore deposit. *Ore Geol. Rev.* **1996**, *11*, 33–51. [[CrossRef](#)]
18. Yi, C.; Gao, H.W.; Li, X.D.; Zhang, K.; Chen, X.L.; Li, J.X. Exploration on the significance of constant element indication for sandstone type uranium deposits of the Zhiluo Formation in northeastern Ordos Basin. *Miner. Depos. Geol.* **2015**, *34*, 801–813.
19. Yang, D.Z.; Xia, B. An Experiment Study on the Role of Organic Materials in Ore-forming of Sandstone-Type Uranium Deposit—A Case Study of the Shihongtan Deposit, Turpan-Hami Basin. *Ore Geol. Rev.* **2004**, *50*, 218–222.
20. Wang, G.R. Oxidization and Migration of Organic Matter in Mineralization of Interlayer Seeping Uranium. *Xinjiang Geol.* **2002**, *20*, 134–136.
21. Zhang, W.H. Experimental Study on the Coordination Role of Humic Acid in Uranium Mineralization Process. Master's Thesis, Northwest University, Xi'an, China, 2006.
22. Cai, Y.G. Experimental Simulation of the Role of Coal-Gas-Oil in Uranium Mineralization. Master's Thesis, Northwest University, Xi'an, China, 2008.
23. He, Z.X.; Fu, J.H.; Xi, S.L.; Fu, S.T.; Bao, H.P. Geological characters of the reservoir in gas field in the Sulige. *J. Oil* **2003**, *24*, 6–12.
24. Quan, Z.G. Classification of interstratigraphic oxide zone boundaries and evaluation of uranium mineralization potential. *Geol. Miner. Search Ser.* **2003**, *4*, 225–228.
25. Yang, R.C.; Han, Z.Z.; Fan, A.P. Sedimentary microphase and stratigraphic stratigraphy of sandstone uranium deposits in the Dongsheng area of Ordos Basin. *J. Stratigr.* **2007**, *31*, 261–266.
26. Miao, A.S.; Jiao, Y.Q.; Chang, B.C.; Wu, L.Q.; Rong, H.; Liu, Z.B. Fine dissection of the ancient interstratified oxide zone of the Dongsheng uranium deposit in northeastern Ordos Basin. *Geol. Sci. Technol. Inf.* **2010**, *29*, 55–61.
27. Zhang, J.D.; Li, Z.Y.; Xu, G.Z. *Significant Progress and Breakthroughs in Uranium Exploration in China—Examples of Newly Discovered and Proven Uranium Deposits since the Entrance of the New Century*, 2nd ed.; Geology Press: Beijing, China, 2015; ISBN 9787116091641.
28. Han, X.Z.; Zhang, Z.L.; Yao, C.L.; Li, X.D.; Li, S.X.; Miao, A.S. Study on uranium mineralization model in the northeast of the Ordos Basin. *Ore Depos. Geol.* **2008**, *27*, 415–421.
29. Jin, R.S.; Miao, P.S.; Sima, X.Z. Structure Styles of Mesozoic-Cenozoic U-bearing Rock Series in Northern China. *Acta Geol. Sin. (Engl. Ed.)* **2016**, *90*, 2104–2116. [[CrossRef](#)]
30. Cheng, Y.H.; Wang, S.Y.; Jin, R.S.; Li, J.G.; Ao, C.; Teng, X.M. Global Miocene tectonics and regional sandstone-style uranium mineralization. *Ore Geol. Rev.* **2019**, *106*, 238–250. [[CrossRef](#)]
31. Cheng, Y.H.; Wang, S.Y.; Li, Y.; Ao, C.; Li, J.G.; Li, H.; Zhang, T. Late Cretaceous–Cenozoic thermochronology in the southern Songliao Basin, NE China: New insights from apatite and zircon fission track analysis. *J. Asian Earth Sci.* **2018**, *160*, 95–106. [[CrossRef](#)]
32. Xia, Y.L.; Lin, J.R.; Liu, H.B.; Fan, G.; Hou, Y.G. Chronology of uranium mineralization in the main uranium basin in north China. *Uranium Geol.* **2003**, *3*, 129–160.
33. Chen, F.Z. Paleo hydrogeological conditions and prospect of uranium mineralization in northern the Ordos Basin. *Uranium Geol.* **2002**, *18*, 287–294.
34. Sun, Y.; Li, Z.Y.; Xiao, X.J.; Hou, G.W. Discuss the relationship between oil and gas trap and uranium mineralization in northern the Ordos Basin. *Uranium Geol.* **2004**, *20*, 337–343.
35. Jin, R.S.; Cheng, Y.H.; Yang, J.; Ao, C.; Li, J.G.; Li, Y.F.; Zhou, X.X. Classification and correlation of Jurassic uranium-bearing series in the Junggar Basin. *Acta Geol. Sin.* **2016**, *90*, 3293–3309.
36. Wu, B.L.; Wang, J.Q.; Liu, C.Y.; Wang, F.Y. Geochemical characters of natural gas geology in the formation of Dongsheng sandstone type uranium ore. *Pet. Nat. Gas Geol.* **2006**, *2*, 225–232.

37. Li, Z.Y.; Fang, X.F.; Chen, A.P.; Ou, G.X.; Xiao, X.J.; Sun, Y.; Liu, C.Y.; Wang, Y. Genesis of gray-green sandstone in sandstone type uranium target layer in northern Ordos Basin. *Chin. Sci. (Ser. D Earth Sci.)* **2007**, *S1*, 139–146.
38. *EJ/T550-2000*; Determination of Uranium in Soil and Rock Samples by Laser-Induced Fluorometry. Commission of Science, Technology and Industry for National Defence of the People's Republic of China: Beijing, China, 2000.
39. *DZ/T0279.27-2016*; Determination of Organic Carbon Contents by Potassium Dichromate Volumetric Method. Ministry of Land and Resources of the People's Republic of China: Beijing, China, 2016.
40. *GB/T6948-2008*; Method of Determining Microscopically the Reflectance of Vitrinite in Coal. Standardization Administration of China: Beijing, China, 2008.
41. Zhuang, X.G.; Yang, S.K.; Zeng, R.S. Characters of Trace Elements in Several Major Coal Producing Areas in China. *Geotech. Inf.* **1999**, *18*, 63–66.
42. The Organic Geochemistry and Sedimentology Laboratory in the Institute of Geochemistry of the Chinese Academy of Sciences. *Organic Geochemistry*, 1st ed.; Science Press: Beijing, China, 1982; ISBN CN13031.3168.
43. Mao, G.Z.; Liu, C.Y.; Zhang, D.D.; Qiu, X.W.; Wang, J.Q.; Liu, B.Q.; Liu, J.J.; Qu, S.D.; Deng, Y.; Wang, F.F.; et al. Experimental study on the role of uranium in the evolution of hydrocarbon generation in type III hydrocarbon rocks. *China Sci. Earth Sci.* **2014**, *44*, 1740–1750.
44. Mao, G.Z.; Liu, C.Y.; Zhang, D.D.; Qiu, X.W.; Wang, J.Q.; Liu, B.Q.; Liu, J.J.; Qu, S.D.; Zhang, S.; Deng, Y.; et al. Influence of uranium on the hydrocarbon evolution of (type II) low-maturity hydrocarbon source rocks. *J. Geol.* **2012**, *86*, 1833–1840.
45. Mao, G.Z.; Liu, C.Y.; Liu, B.Q.; Zhang, D.D.; Qiu, X.W.; Wang, J.Q. Influence of uranium on the evolution of hydrocarbon generation in type I low-maturity hydrocarbon source rocks. *J. China Univ. Pet. (Nat. Sci. Ed.)* **2012**, *36*, 172–181.
46. Wu, B.L. Geology and Mineralization of Sandstone Type Uranium Ore in the Middle Cenozoic Basin of Northwest China. Ph.D. Thesis, Northwest University, Xi'an, China, 2005.
47. Yang, D.Z. *Organic Geochemistry of Uranium in the Southwestern Jurassic of the Tuha Basin*; Beijing Institute of Geology of Nuclear Industry: Beijing, China, 2002.
48. Li, S.F.; Zhang, Y. Formation mechanism of uranium minerals at sandstone-type uranium deposits. *Uranium Geol.* **2004**, *20*, 81–84.

Disclaimer/Publisher's Note: The statements, opinions and data contained in all publications are solely those of the individual author(s) and contributor(s) and not of MDPI and/or the editor(s). MDPI and/or the editor(s) disclaim responsibility for any injury to people or property resulting from any ideas, methods, instructions or products referred to in the content.